

Efficient photonic crystal Y-junctions

Rab Wilson¹, Tim J Karle¹, I Moerman² and Thomas F Krauss^{1,3}

¹ School of Physics and Astronomy, University of St Andrews, North Haugh, St Andrews, Fife KY16 9SS, UK

² University of Gent, IMEC, Department of Information Technology, Sint-Pieternieuwstraat, 41 B-9000 Gent, Belgium

Received 24 October 2002, in final form 20 February 2003

Published 25 June 2003

Online at stacks.iop.org/JOptA/5/S76

Abstract

A highly efficient Y-junction based on a planar photonic crystal (PhC) platform is presented. The PhC consists of a triangular array of holes etched into a GaAs/AlGaAs heterostructure, with a typical period of 322 nm and ~35% fill factor. The Y-junction has smaller holes positioned at the centre of the junction, giving rise to very uniform splitting and high transmission. The performance is very encouraging, with experimental transmission of approximately 40% for each arm of the Y-splitter relative to a comparable single-defect PhC waveguide.

Keywords: Photonic crystals, photonic integrated circuits, semiconductor optoelectronics

1. Introduction

Photonic crystals (PhC) have the potential to provide ultracompact photonic components that will enable the miniaturization of optical circuits and promise to revolutionize integrated optics. Primarily, such devices operate in the photonic band gap (PBG) of the periodic dielectric structure, which allows tight confinement of light to predetermined pathways in order to route and control it through the circuit. As the crystal dimensions are on a wavelength scale, integrated optical circuits with packing densities exceeding four orders of magnitude higher than those currently achieved can be realized.

Most theoretical studies conducted so far have investigated arrays of dielectric rods in air. The advantage of this model system is that waveguides created by removing a single line of rods are single moded. Getting light to travel around sharp bends with high transmission is then relatively straightforward, and T-junctions and Y-junctions have already been proposed [1]. Unfortunately, the 'rods in air' approach does not provide sufficient vertical confinement and is difficult to implement for most practically useful device implementations in the optical regime. A slab waveguide structure, consisting of air holes etched into a dielectric medium, such as a GaAs/AlGaAs heterostructure [2] or a semiconductor membrane [3–5], remedies this problem and allows waveguides with tolerable losses to be realized. The problem encountered for the 'holes in dielectric' approach is that the single-defect PhC waveguide becomes multi-moded, which makes it difficult to get light to flow efficiently around the circuit because

higher-order modes are easily excited at discontinuities [5–7]. Whereas straight waveguides and bends have been studied by many groups, the very important problem of junctions that is essential for the operation of more complex circuits has only recently received attention [8–11]. The most straightforward Y-splitter design consists of three single-defect ('W1') waveguides joined together at 120°, which leads to strong reflections and narrow-bandwidth operation [10]. An alternative design, based on a triple-line-defect waveguide [11], improves performance significantly because the waveguides used are inherently monomode. Here, we present the first demonstration of efficient light propagation through a Y-junction based on the more commonly used W1 waveguide geometry.

2. Fabrication and characterization

The devices were fabricated in a GaAs/AlGaAs heterostructure grown by MOCVD. The layer structure consists of a 400 nm GaAs core with 100 nm of 25% AlGaAs cladding on both sides, placed on top of a 1.5 μm thick 60% AlGaAs buffer. The PhC had a lattice period of $a = 322$ nm with approximately 200 nm diameter holes, which translates to a fill factor of 35%. Due to the nature of the etching process, however, some lateral expansion of the hole may occur towards the bottom of the holes, thereby increasing the effective fill factor. Structures were written by electron-beam lithography on a LEICA EBPG5 Beamwriter (at Glasgow University, UK) and etched to a depth of 1.2 μm by reactive ion etching using SiCl_4 and a silica mask. For comparison, we fabricated three types of device (see figure 1): a 3 μm wide ridge waveguide, a single-defect

³ Author to whom any correspondence should be addressed.

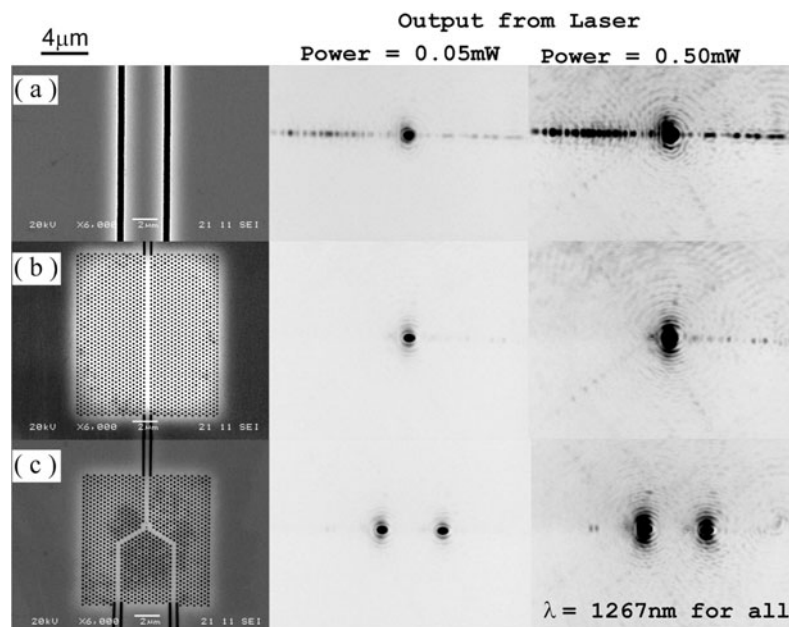


Figure 1. SEM micrographs of (a) a 3 μm wide waveguide, (b) a W1 waveguide and (c) a Y-junction. Alongside each micrograph is an image of the output facets captured using an IR camera. For comparison and to eliminate effects arising from the nonlinear response of the Vidicon camera, two images for each structure are provided, the first using low power from the laser (0.05 mW) while the other was at a higher power (0.5 mW). The wavelength for all images was $\lambda = 1267\text{ nm}$. The images show TE_{00} -like modes at the output facet, indicating single-mode propagation through the entire device.

PhC waveguide (W1) and a Y-splitter. The PhC-based devices were based on 32-by-32 unit cells, i.e. only 10 μm by 10 μm in size. The input waveguides were adiabatically tapered from a 3 to 0.54 μm width to keep lateral mode mismatch between the ridge waveguide and the PhC waveguide to a minimum. The peak transmission of a W1, approximately 63% of that for a 3 μm broad ridge waveguide, was used as a reference for comparison with the Y-splitter. This type of normalization should accommodate extrinsic effects such as laser–waveguide coupling and the modal mismatch between the ridge and the PhC waveguide. Figure 1 provides a graphic illustration of the high transmission through these device structures.

In the design process and for comparison with experimental results, we use 2D finite-domain–time–domain (FDTD) simulation (Fullwave by RSoft Incorporated) with a fill factor of 35%. An effective refractive index of $n_{eff} = 3.04$ for our slab structure is used that was derived empirically from previous experiments, which were conducted by our group for PhC devices using the above heterostructure for PhC structures fabricated at Glasgow. Our measurement set-up consists of a semiconductor laser with a tunable wavelength range extending from 1255 to 1365 nm, modulated at 333 Hz and scanned with a step size of 0.05 nm. A Ge pn photodetector in conjunction with a lock-in amplifier is used for the detection of the transmitted light. The light is launched with a $\times 60$ lens and captured with a $\times 40$ microscope objective. A Wollaston prism ensures that only TE-like polarization is transmitted. A Vidicon camera allows us to check the mode profile at the output facet of the devices (figure 1). A characteristic feature of the transmission measurements is the presence of Fabry–Perot interference fringes. The transmitted intensity for a Fabry–Perot resonator having mirrors with different reflectivity, ignoring absorption and loss, is given by

$$I_t = \frac{(1 - R_1)(1 - R_2)}{1 + (1 - \sqrt{R_1 R_2})^2 + 4\sqrt{R_1 R_2} \sin^2\left(\frac{\delta}{2}\right)}.$$

The phase δ is given by $\delta = (4n_{eff}d/\lambda)$ for a given wavelength λ , where n_{eff} is the effective refractive index of the ridge waveguide and d would be the distance between the mirrors. Maximum transmission occurs when $\delta = 2\pi$, implying that the peaks of the oscillations represent the true transmission, as the transmission of a Fabry–Perot resonator with 0% mirror reflectivity would be 100% throughout. The whole test piece can be considered as set of multiple cavities, which produce oscillating spectral features in the transmission measurements (figure 2) caused by reflections at the cleaved facets of the input and output waveguides in conjunction with the PhC structure positioned in the middle of the sample. The finite reflectivity reduces transmission when a wavelength is not resonant a cavity. For our sample the data from one branch of the Y-splitter show a Fabry–Perot interference fringes with a period of $\sim 0.55\text{ nm}$, which translates to $\sim 0.48\text{ mm}$. This is the approximate length of the input and output ridge waveguides to the device; because the input and output waveguides are not exactly the equal in length, the Fabry–Perot interference fringes observed in the inset in figure 2 is a superposition of two of the Fabry–Perot interference fringes from these two cavities. The other low-frequency perturbation corresponds to the PhC Y splitter.

3. Results and discussion

Figure 1 beautifully demonstrates the efficiency of the devices despite the nonlinear response of the Vidicon camera used for image capture. The negative images clearly show single-mode

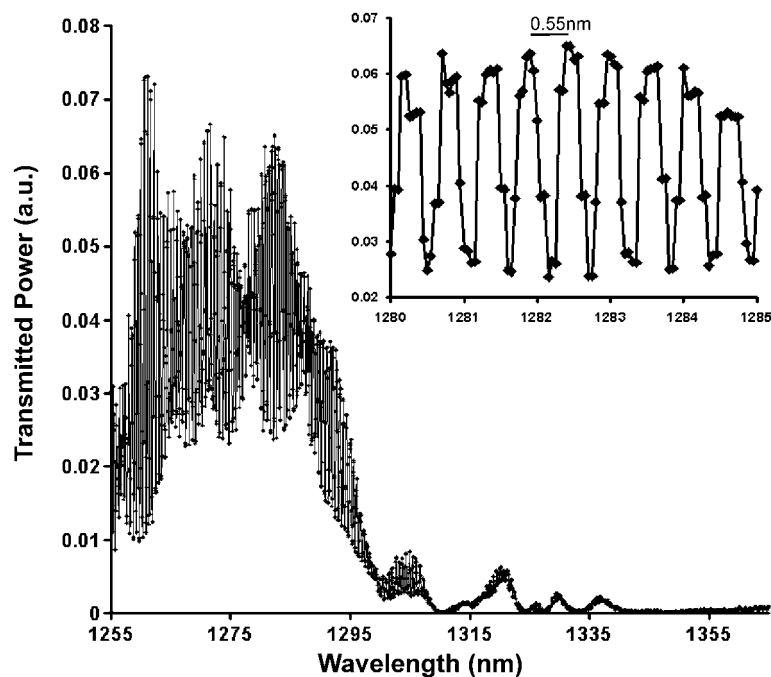


Figure 2. This shows the transmission data from the RHS branch of the Y-splitter and the Fabry–Perot interference fringes with a period of ~ 0.55 nm (inset). This gives d as ~ 0.48 nm, which is the length of the ridge from the waveguide to the device. The other low-frequency perturbation corresponds to the PhC Y-splitter.

propagation, as well as transmission almost as high as in a $3\ \mu\text{m}$ waveguide and a good balance between the two branches of the Y-junction.

The essential function of a W1 PhC Y-splitter is to convert a single-mode train in the input waveguide symmetrically into two single-mode trains in the output waveguides. The SEM shown in figure 3(a) illustrates the construction of our design. A small hole is placed on a lattice site immediately in front of a single-defect PhC waveguide so as to perturb the incoming mode as gently as possible when dividing it in two. Palamaru and Lalanne originally proposed the use of such small holes as a method for mode matching between ridge waveguides and PhC waveguides [12]. They showed that a small hole, followed by a line of holes gradually increasing in size, could adiabatically convert a conventional waveguide mode into a PhC waveguide mode without incurring any significant loss in transmission. In a similar way, we achieved near-adiabatic splitting of the single input mode into two output modes by gradually varying the size of the holes at the junction. The size of the initial hole was designed to be $0.5r$ and the second $0.75r$. As shown by the SEM micrograph of the junction (figure 3(a)), these holes turned out slightly smaller ($0.4r$ and $0.68r$, respectively) in the actual experiment. Due to the nature of the RIE process (‘RIE lag’) the smaller holes will not be etched as deeply as the full-size holes in the lattice, thereby introducing a potential source of loss, i.e. scattering into the substrate. As predicted in [12], very little loss arises from these smaller holes, however, a fact we have now confirmed experimentally. Comparison of the experimental data with the 2D FDTD model (figure 4) shows a remarkable agreement as regards transmitted power, as the 2D FDTD model completely ignores out-of-plane scattering losses. The good agreement between model and experiment clearly implies that the real out-of-plane loss must be below the experimental detection limit.

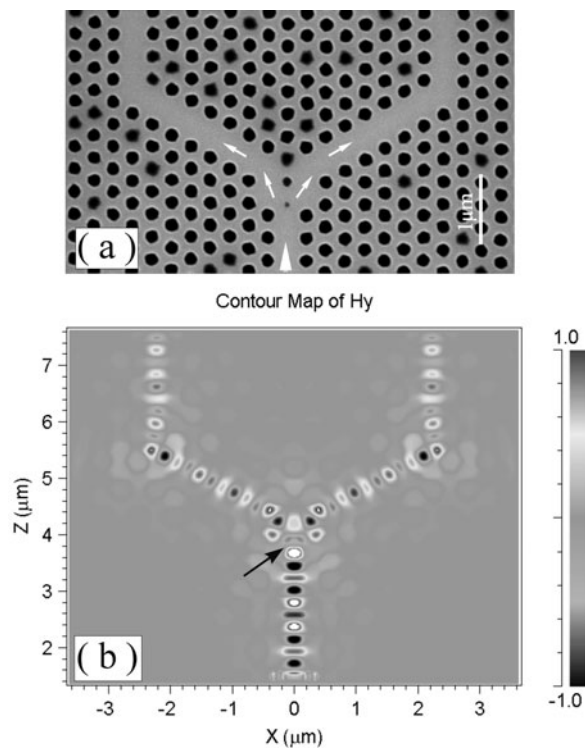


Figure 3. (a) A close-up view of the Y-junction. The arrows indicate the light path through the junction. The important point to note is the size of the holes, which are used to adiabatically split the incoming single mode into two single modes entering the output ports. (b) A two-dimensional FDTD simulation of propagation through the Y-junction. The arrow indicates the splitting of an incoming single mode by the small hole.

In essence, the net effect of introducing additional holes at the junction is to reduce the volume of the intersection, thereby

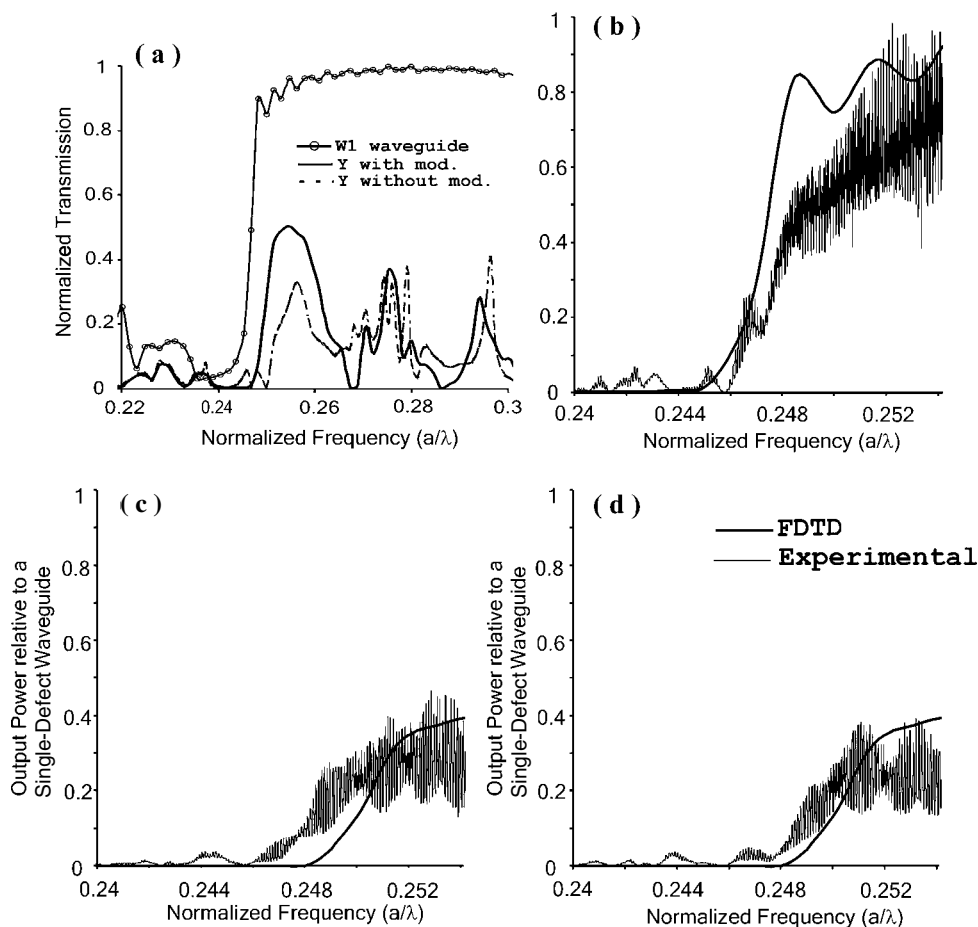


Figure 4. (a) The FDTD calculation to compare the transmission bandwidth and power transmission of a Y-junction, with and without modification, to that of a W1 waveguide. ((b)–(d)) Comparison of experimental and simulated (2D FDTD) power transmissions for a W1 waveguide (b) and the left (c) and right (d) arms of the Y-junction. The Y-junction data are normalized to the maximum transmission obtained through a W1 waveguide, so the vertical scales in (b)–(d) are identical.

preventing expansion into a higher-order mode. Boscolo *et al* [8] showed that poor transmission can originate from modal mismatch at the junction. If the incoming mode has space to expand in the junction area, it excites a higher mode with odd parity that is either very lossy or cannot propagate in the output waveguides, so most of the incoming light is reflected and transmission is poor. Therefore, the excitation of modes with odd parity would act as a loss mechanism for the Y-junction. Placing additional holes at the junction then clearly increases the bandwidth and power transmission, as directly observed in our comparative simulations of a Y-junction with and without modifications (figure 4(a)). This solution is similar to an independent proposal given by Chutinan *et al* [9] who numerically studied the use of small holes placed in the centre of a W1 in order to increase the transmission of a 60° bend.

In figure 4, we present calculated and measured spectra for the W1 waveguide and Y-splitter structures in order to highlight the high transmission achieved. The maximum transmission values for the W1 and Y-splitter agree extremely favourably with the simulations, although the position of the band edge is slightly shifted with respect to the calculated spectra. Our observations confirm those of Chutinan and Noda [7, 13] who show that for a suitable choice of effective refractive index,

2D simulations give the same quantitative characteristics as 3D simulations.

The Y-splitter shows useful transmission over a 40 nm range, which is at least double that reported for an unmodified junction (figure 3(a)) [10] and similar to that reported for the Y-junction based on triple-defect waveguides [11]. The maximum power transmission is approximately 40% in both arms, demonstrating well-balanced device operation.

To summarize, we have demonstrated a functional Y-splitter with excellent performance based on a W1 PhC waveguide in the ‘air holes in dielectric’ geometry. High power transmission of up to 84% ($Y_{left} + Y_{right}$) relative to a W1 waveguide was observed. The key feature of the device is the addition of smaller holes at the centre of the junction in order to avoid mode expansion and excitation of higher-order modes at the output ports.

Acknowledgments

We wish to acknowledge the EU-IST project ‘Photonic Integrated Circuits using Crystal Optics (PICCO)’ for funding of this work. The authors would also like to thank the Nanoelectronics Research Centre at Glasgow University for technical support. TFK is supported by a Royal Society University Research Fellowship.

References

- [1] Fan S H, Johnson S G, Joannopoulos J D, Manolatos C and Haus H A 2001 Waveguide branches in photonic crystals *J. Opt. Soc. Am. B* **18** 162–5
- [2] Krauss T F, De la Rue R M and Brand S 1996 Two-dimensional photonic-bandgap structures operating at near infrared wavelengths *Nature* **383** 699–702
- [3] Loncar M, Nedeljkovic D, Doll T, Vuckovic J, Scherer A and Pearsall T P 2000 Waveguiding in planar photonic crystals *Appl. Phys. Lett.* **77** 1937–9
- [4] Chow E, Lin S Y, Johnson S G, Villeneuve P R, Joannopoulos J D, Wendt J R, Vawter G A, Zubryski W, Hou H and Alleman A 2000 Three-dimensional control of light in a two-dimensional photonic crystal slab *Nature* **407** 983–6
- [5] Notomi M, Shinya A, Yamada K, Takahashi J, Takahashi C and Yokohama I 2001 Singlemode transmission within photonic bandgap of width-varied single-line-defect photonic crystal waveguides on SOI substrates *Electron. Lett.* **37** 293–5
- [6] Talneau A, Le Gouezigou L, Bouadma N, Kafesaki M, Soukoulis C M and Agio M 2002 Photonic-crystal ultrashort bends with improved transmission and low reflection at 1.55 μm *Appl. Phys. Lett.* **80** 547–9
- [7] Chutinan A and Noda S 2000 Waveguides and waveguide bends in two-dimensional photonic crystal slabs *Phys. Rev. B* **62** 4488–92
- [8] Boscolo S, Midrio M and Krauss T F 2002 Y junctions in photonic crystal channel waveguides: high transmission and impedance matching *Opt. Lett.* **27** 1001–3
- [9] Chutinan A, Okano M and Noda S 2002 Wider bandwidth with high transmission through waveguide bends in two-dimensional photonic crystal slabs *Appl. Phys. Lett.* **80** 1698–700
- [10] Sugimoto Y, Ikeda N, Carlsson N, Asakawa K, Kawai N and Inoue K 2002 Light-propagation characteristics of Y-branch defect waveguides in AlGaAs-based air-bridge-type two-dimensional photonic crystal slabs *Opt. Lett.* **27** 388–90
- [11] Lin S Y, Chow E, Bur J, Johnson S G and Joannopoulos J D 2002 Low-loss, wide angle Y splitter at 1.6 μm wavelengths built with a two-dimensional photonic crystal *Opt. Lett.* **27** 1400–2
- [12] Palamaru M and Lalanne P 2001 Photonic crystal waveguides: out-of-plane losses and adiabatic modal conversion *Appl. Phys. Lett.* **78** 1466–8
- [13] Painter O, Vuckovic J and Scherer A 1999 Defect modes of a two-dimensional photonic crystal in an optically thin dielectric slab *J. Opt. Soc. Am. B* **16** 275–85